A R C H I V E S O F M E T A L L U R G Y A N D M A T E R I A L S
Volume 60 2015 Issue 2
DOI: 10.1515/amm-2015-0158

S.H. LEE*, B. AHN*,♯

EFFECT OF COMPACTION PRESSURE AND SINTERING TEMPERATURE ON THE LIQUID PHASE SINTERING BEHAVIOR OF Al-Cu-Zn ALLOY

WPŁYW CIŚNIENIA PRASOWANIA I TEMPERATURY SPIEKANIA NA SPIEKANIE STOPU Al-Cu-Zn Z UDZIAŁEM FAZY CIEKŁEJ

The liquid phase sintering characteristics of Al-Cu-Zn alloy were investigated with respect to various powder metallurgy processing conditions. Powders of each alloying elements were blended to form Al-6Cu-5Zn composition and compacted with pressures of 200, 400, and 600 MPa. The sintering process was performed at various temperatures of 410, 560, and 615°C in N_2 gas atmosphere. Density and micro-Vickers hardness measurements were conducted at different processing stages, and transverse rupture strength of sintered materials was examined for each condition, respectively. The microstructure was characterized using optical microscope and scanning electron microscopy. The effect of Zn addition on the liquid phase sintering behavior during P/M process of the Al-Cu-Zn alloy was also discussed in detail.

Keywords: powder metallurgy, liquid phase sintering, compaction pressure, Al-Cu-Zn alloy

1. Introduction

Recently, the application of aluminum and its alloy has been significantly expanded in the automotive industries because of increased demand for light weight structural parts to reduce fuel consumption [1, 2]. Especially, Al powder metallurgy (P/M) offers the following advantages: (i) improvement of mechanical properties and corrosion resistance, (ii) reduction of manufacturing cost, and (iii) production of near net-shaped components [3-5]. However, the sinterability of Al and its alloys still need to be improved for wide application of Al P/M products. One of the factors affecting the lower sinterability of P/M Al is very stable Al_2O_3 layer in thickness of 50~150Å on surface of water-atomized Al powders [6, 7]. However, this oxide layer cannot be removed easily, resulting in limitation of mass flow between powder particles during sintering and in degradation of mechanical properties [8].

One of the approaches to improve the sinterability of P/M Al is to add proper alloying elements, such as Cu, Mg, Zn, or Si, to create a liquid phase during sintering, called as liquid phase sintering (LPS) [9]. During sintering, localized alloying occurs at interface between Al powders and alloying elements forming a liquid phase, and the liquid phase can infiltrate between powder particles improving the adhesion of powders [10, 11]. In the present study, Al-Cu-Zn alloy system was used, since both Cu and Zn form liquid phases with Al. Cu element in Al matrix forms Al-Cu liquid phase at temperature of 548°C, while Zn element forms Al-Zn liquid phase at 380°C which is lower than the Al-Cu liquid phase [12].

Compaction pressure is also one of the factors that must be considered for the sinterability of P/M alloys. The range of compaction pressures can be divided into three different regions depending on the deformation of powders during compaction: (i) elastic deformation region below 94% green density relative to theoretical density (T.D.), (ii) local plastic deformation region in the range of 94~97% T.D., and (iii) plastic deformation region above 97% T.D. [13]. In the plastic deformation region, internal pores after compaction are primarily closed ones, however, those can be filled by liquid phase during sintering, resulting in improved sinterability.

2. Experimental

Water atomized Al powder, electrolytic processed Cu powder, and pre-alloyed Al-20Zn (wt.%) powder were mixed to form the final composition of Al-6Cu-5Zn (wt.%), and blended using a 3D tubular mixer for 60 min. Mean particle sizes of Al, Cu, and pre-alloyed Al-Zn powders were 150, 45, and 45 μm, respectively. The blended powder was compacted with three different pressures (200, 400, and 600 MPa). Die-wall lubrication was employed for each compaction stroke using Ethylene Bis Stearamide (EBS) lubricant. Green compacts were sintered at three different temperatures (410, 560, and 615°C) in pure N_2 gas. During the sintering, the green compacts were heated in the rate of 10°C/min and held at sintering temperatures for 5 min (410 and 560°C) and for

* DEPARTMENT OF ENERGY SYSTEMS RESEARCH, AJOU UNIVERSITY, SUWON, KOREA
♯ Corresponding author: byungmin@ajou.ac.kr

60 min (615°C), and then all compacts were immediately water-quenched, as shown in Fig. 1.

Microstructural characterization was conducted using an optical microscope (OM) and a field emission scanning electron microscope (FE-SEM). The compositional analysis was performed using an energy-dispersive X-ray spectroscopy (EDS). To evaluate sintered properties of materials processed with different compaction pressures and different sintering temperatures, density measurements, micro-Vickers hardness measurements, and transverse rupture strength (TRS) using a universal testing machine were performed.

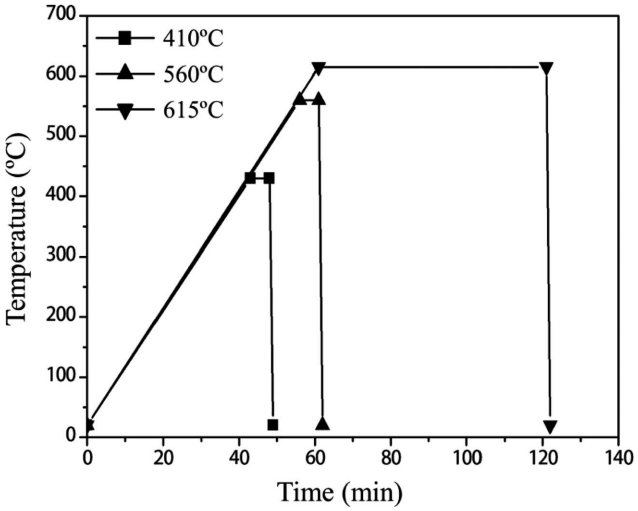

Fig. 1. Schematic of the sintering cycle for Al-6Cu-5Zn alloy (holding time: 5 min at 410 and 560°C, 60 min at 615°C)

3. Results and discussion

Fig. 2 shows density variations depending on both compaction pressures and sintering temperatures. The density increases as compaction pressure increases at virtually all sintering temperatures in addition to the green compacts. For all compaction pressures, the overall trend of density variations depending on sintering temperatures was uniform. When the powder compacts were sintered at 410°C, the density negligibly varied from the green density regardless of compaction pressures, because no diffusion interactions occurred at that temperature. However, when sintered at 560°C, the density was significantly decreased for all compaction pressures, attributed to the expansion of volume. At this temperature, Al-Zn and Cu elements form small amount of liquid phase with Al, and the diffusion from the liquid to solid phase expands interparticle distance forming unfilled skeleton of the powder body, resulting in the increase of volume [14-17]. When sintered at 615°C, in which LPS actively occurs in addition to solid state sintering, the density increases compared to that achieved at 560°C because of the volume shrinkage by dissolution of solid into the liquid phase. In comparison of sintered density between 560 and 615°C: (i) at lower compaction pressure of 200 MPa, the increment of density was significant from 560 to 615°C because an amount of pores were filled by liquid phase during sintering, (ii) at higher compaction pressure of 600 MPa, on the contrary, the increase in density was negligible because of relatively small amount of existing pores filled by the liquid phase.

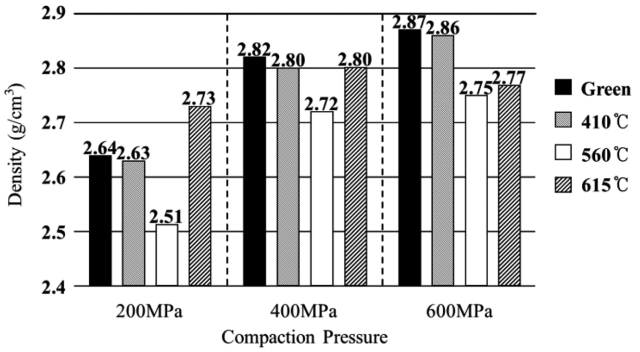

Fig. 2. Density variation depending on the compaction pressures and sintering temperatures

The microstructural variation depending on the sintering temperatures is shown in Fig. 3 when compacted at 400 MPa. At 410°C in Fig. 3a, pre-alloyed Al-20Zn powder was found non-dissolved condition, although the temperature was higher than the Al-Zn eutectic point of 380°C. The absence of diffusion interaction in Al-Zn phase at 410°C is attributed to the rise in melting temperature to about 550°C with the presence of pre-alloyed powder. Both materials sintered at 560 and 615°C exhibits the liquid phase formed at particle boundaries, as shown with white arrows in Fig. 3b and 3c, respectively. However, the material sintered at 560°C appears to contain un-filled pores, as shown with yellow dotted lines in Fig. 3b, which corresponds well with the density result in Fig. 2. The material sintered at 615°C contains no large pores, and the liquid phase migrated to the particle boundaries resulting in the higher density.

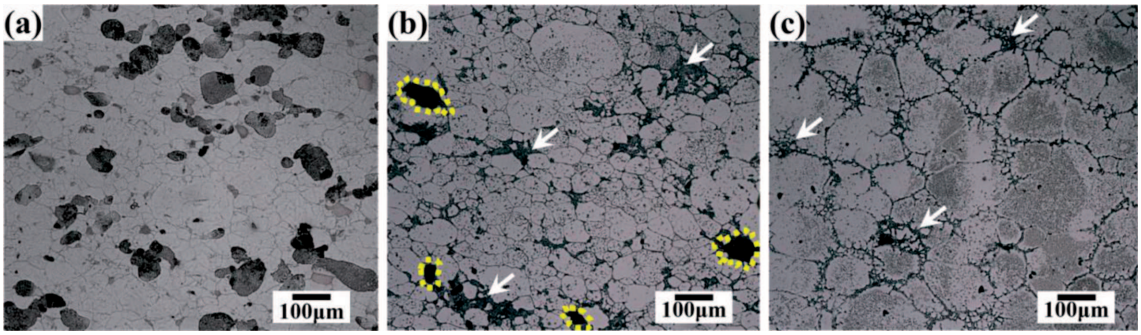

Fig. 3. Optical micrographs of materials compacted at 400 MPa after sintering at temperatures of (a) 410, (b) 560, and (c) 615°C. The white arrows and yellow dotted lines indicate liquid phase and unfilled pores, respectively

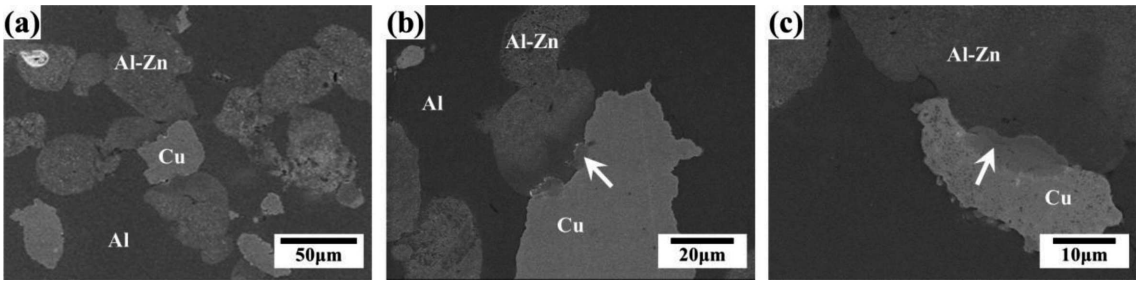

Fig. 4. BSE micrographs of materials sintered at 410°C with compaction pressures of (a) 200, (b) 400, and (c) 600 MPa. The arrows indicate partial diffusion between Al-Zn and Cu powders

To evaluate the LPS behavior in detail, overall microstructures of the Al-6Cu-5Zn alloy are compared in Fig. 4~6. Fig. 4 shows a set of backscattered electron (BSE) SEM micrographs representing microstructural variation with respect to the compaction pressures when sintered at 410°C. Regardless of the compaction pressure, all three components, Al matrix, Cu powder, and pre-alloyed Al-Zn powder were found in undissolved condition, as shown in Fig. 4a as black, white, and gray regions, respective. This result indicates that no substantial diffusion reaction occurred at that temperature, as discussed above in Fig. 3a. However, detailed microstructural investigation using SEM shows an evidence of partial diffusion between Al-Zn and Cu powders when compacted at 400 and 600 MPa as shown in Fig. 4b and 4c. The arrows in Fig. 4b and 4c indicate such diffusion regions appeared with different contrast in SEM images at the interface between Al-Zn and Cu powders. The occurrence of partial diffusion at relatively high compaction pressures is attributed to the increase of mechanical interlock in contact surfaces between powder particles [18].

Fig. 5 shows another set of SEM images from the materials sintered at 560°C representing microstructural variation depending on the compaction pressures. For all compaction pressures, it is apparent that a small amount of liquid phase was formed and appeared to fill into the interparticle boundaries, as shown as brighter regions indicated with arrows in Fig. 5. The elemental analysis using EDS confirmed the liquid phase at 560°C in all three materials consists of virtually same compositions of Al, Cu, and Zn, although the EDS result is not shown in this article. At relatively higher compaction pressures of 400 and 600 MPa, some closed pores were found in Fig. 5b and 5c. In general, as compaction pressure increases, powder particles are more plastically deformed. Therefore, interparticle porosity is isolated because of the polyhedral interlocking between particles subject to severe compaction, and then the porosity develops into the closed pores.

Fig. 6 shows the final set of SEM images from the materials sintered at 615°C. The formation of liquid phase is clearly observed at all compaction pressures. It appears that the liquid phase successfully filled into the interparticle boundaries at relatively lower pressures of 200 and 400 MPa, as shown as brighter regions in Fig. 6a and 6b. However, at 600 MPa in

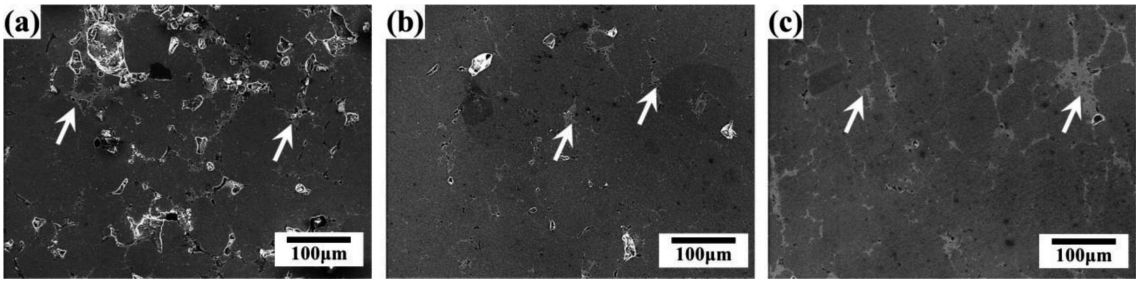

Fig. 5. BSE micrographs of materials sintered at 560°C with compaction pressures of (a) 200, (b) 400, and (c) 600 MPa. The arrows indicate LPS regions

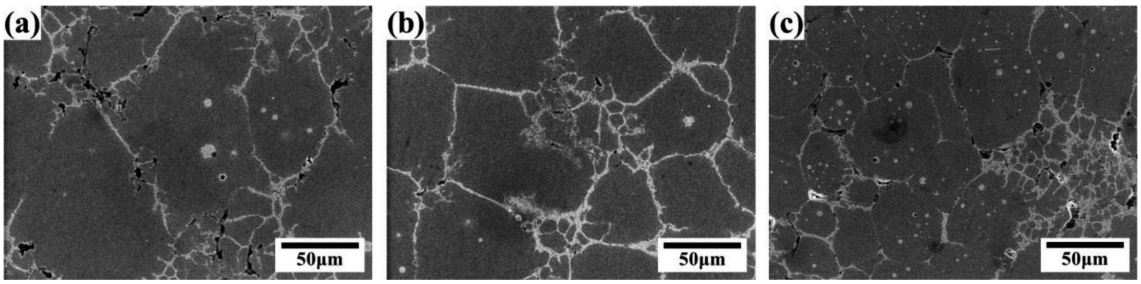

Fig. 6. BSE micrographs of materials sintered at 615°C with compaction pressures of (a) 200, (b) 400, and (c) 600 MPa

Fig. 6c, the narrow regions of particle boundaries significantly hindered the flow of liquid phase, resulting in the limited presence of liquid phase. The closed pores also exist in the material compacted at 600 MPa, which remain unfilled by the liquid phase. These isolated closed pores are hardly filled by the liquid phase during sintering because of the limited mobility, causing decrease in density and mechanical properties at extremely high compaction pressure.

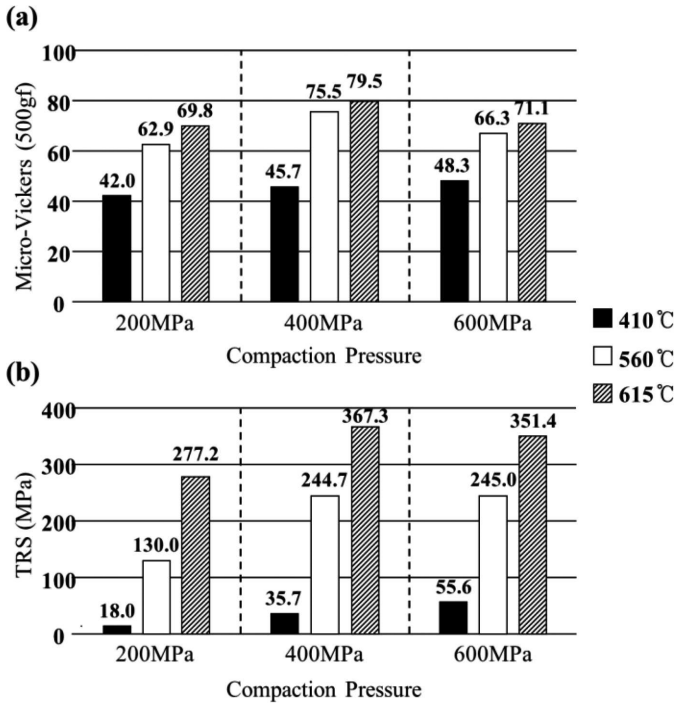

Fig. 7. Variation of micro-Vickers hardness and TRS depending on the compaction pressures and sintering temperatures

To investigate the effect of both compaction pressures and sintering temperatures on the mechanical behavior, the micro-Vickers hardness and TRS were measured, as shown in Fig. 7. At all compaction pressures, both hardness and TRS increased as sintering temperature increases, because the bonding energy between powder particles increases with temperature. The increment of both hardness and TRS from 410 to 560°C is relatively more significant compared with that from 560 to 615°C. As discussed above, it is evident that the LPS is initiated in addition to the solid state sintering at 560°C, whereas virtually no sintering reaction occurred at 410°C. Such different sintering behavior leads to the significant increase of mechanical behavior. The greatest hardness and TRS values were achieved at 615°C sintering and 400 MPa compaction pressure. This result is attributed to an appropriate combination between the sintering temperature and compaction pressure.

4. Conclusions

1. Al-6Cu-5Zn P/M alloy was investigated in the present study to examine the influence of compaction pressures and sintering temperature on its liquid phase sintering (LPS) behavior. A combination of three compaction pressures (200, 400, and 600 MPa) and three sintering temperatures (410, 560, and 615°C) leads to the following conclusions.
2. To evaluate the effect of sintering temperature, when the alloy powder was compacted at 400 MPa, the LPS didn't take place at 410°C but occurred at 560°C and above. At the initial stage of LPS at 560°C, small amount of liquid phase expanded the total volume of powder compact so that the density decreased. However, when sintered at 615°C, the density increased because of pore-filling effect by the liquid phase.
3. To evaluate the effect of compaction pressures, when sintered at 410°C, no diffusion reaction occurred with compaction pressure of 200 MPa while partial diffusion took place with the pressures of 400 and 600 MPa because of enhanced interlocking between powder particles at higher compaction pressures. When sintered at 560°C, the LPS occurred to a small extent for all compaction pressures. When sintered at 615°C, sufficient LPS took place for all compaction pressures, however, the material compacted at 600 MPa appeared to contain closed pores which remain unfilled by the liquid phase, causing decrease in density and mechanical properties. Indeed, compaction with higher pressure significantly limits the flow of liquid phase during sintering because of the presence of closed pores.
4. The greatest mechanical behavior was achieved when the alloy powder was compacted at 400 MPa and sintered at 615°C, attributed to an appropriate trade-off between the compaction of powder and the flow of LPS.

Acknowledgements

This research was supported by the Basic Science Research Program through the National Research Foundation of Korea (NRF) funded by the Ministry of Science, ICT & Future Planning (MSIP) of Korean government (Grant No. 2012R1A1A1012983).

REFERENCES

[1] A. Gokce, F. Findik, A.O. Kurt, Materials Characterization **62**, 730-735 (2011).
[2] B. Legendre, Y. Feutelais, J.M. SanJuan, I. Hurtado, Journal of Alloys and Compounds **308**, 216-220 (2000).
[3] L. Kovarik, S.A. Court, H.L. Fraser, M.J. Mills, Acta Materialia **56**, 4804-4815 (2008).
[4] G.B. Schaffer, Materials Forum **28**, 65-74 (2004).
[5] S. Szczepanik, T. Sleboda, Journal of Materials Processing Technology **60**, 729-733 (1996).
[6] G.B. Schaffer, B.J. Hall, Metallurgical and Materials Transactions A **33**, 3279-3284 (2002).
[7] E.J. Lavernia, J.D. Ayers, T.S. Srivatsan, International Materials Reviews **37**, 1-44 (1992).
[8] R.Q. Guo, P.K. Rohatgi, D. Nath, Journal of Materials Science **32**, 3971-3974 (1997).
[9] R.M. German, Liquid phase sintering, Plenum Press, New York (1985).
[10] G.B. Schaffer, T.B. Sercombe, R.N. Lumley, Materials Chemistry and Physics **67**, 85-91 (2001).
[11] J.M. Martin, F. Castro, Journal of Materials Processing Technology **143-144**, 817-820 (2003).
[12] H. Liang, Y.A. Chang, Journal of Phase Equilibria and Diffusion **19**, 25-37 (1998).

[13] R.W. Heckel, Transactions of the Metallurgical Society of AIME **221**, 671-675 (1961).
[14] J.L. Johnson, R.M. German, Metallurgical and Materials Transactions B **27B**, 901-909 (1996).
[15] R.M. German, P. Suri, S.J. Park, Journal of Materials Science **44**, 1-39 (2009).
[16] N.D. Lesnik, Powder Metallurgy and Metal Ceramics **51**, 639-656 (2013).
[17] G.N. Romanov, Russian Journal of Non-Ferrous Metals **51**, 347-351 (2010).
[18] M.F. Moreno, C.J.R. GonzalezOliver, Powder Technology **245**, 13-20 (2013).

Received: 20 November 2014.